

# Inner Current Controls of Grid-Connected PV for Unbalanced Grid Conditions

Abdulhakim Alsaiif

Smart Grid Power Systems Lab  
Department of Electrical Engineering  
University of South Florida  
Tampa, FL 33620, USA  
alsaiif1@usf.edu

Zhixin Miao

Smart Grid Power Systems Lab  
Department of Electrical Engineering  
University of South Florida  
Tampa, FL 33620, USA  
zmiao@usf.edu

Lingling Fan

Smart Grid Power Systems Lab  
Department of Electrical Engineering  
University of South Florida  
Tampa, FL 33620, USA  
linglingfan@usf.edu

**Abstract**—This paper examines the implementation and performance of unbalance controls in a grid-connected converter of a solar photovoltaic (PV) power plant. While the objectives of the outer control loops include DC-link voltage regulation and AC voltage regulation, the inner current controls are designed to track the current orders including positive- and negative-sequences generated by the outer controls and also to mitigate second harmonic ripples in real power. Two types of inner current controls, namely, decoupled double synchronous reference frame (DDSRF), and proportional-resonant (PR) control, are implemented. An overview of these current control techniques is first provided. Comparison of performance is then conducted in electromagnetic transient (EMT) testbeds built in MATLAB/SimScope environment.

**Index Terms**—Voltage source converter (VSC); grid-connected; unbalance control; solar photovoltaic (PV) grid integration; double frequency mitigation.

## I. INTRODUCTION

REAL-WORLD field recorded data show that grid-connected solar PVs are designed to suppress negative-sequence current injection into the grid during unbalanced grid conditions [1]. This type of design usually sets the negative-sequence current order in a grid-connected voltage-source converter (VSC) to be zero. On the other hand, this design results in ripples of twice the fundamental grid frequency in the total instantaneous power due to the interaction of the positive-sequence current injection and negative-sequence grid voltage. A more sophisticated design to mitigate ripples in power is desired by regulating both the positive- and negative-sequence currents. Such idea has been explored in the literature for VSC control using double reference frames, e.g., [2].

On the other hand, the VSC control system discussed in [2] is in PQ regulation mode. For solar PV's grid-connected converters, outer loop controls, DC-link and AC voltage regulation, are much more common. Thus, the significance of the current paper is to implement unbalance control into solar PV's grid-connected converters to achieve DC-link voltage and AC voltage regulations, and to mitigate ripples in the DC voltage and the total three-phase power begin delivered into the grid.

There are a variety of methods of unbalance control. The double synchronous reference frame (DSRF) control is an effective method to regulate positive- and negative-sequence cur-

rents, based on two control loops using PI controllers [3], [4]. The decoupled DSRF (DDSRF) is an improved DSRF that applies its decoupled network to eliminate double frequency ( $2\omega$ ) oscillations from each sequence transformed  $dq$  currents [5]. Another control scheme for unbalanced currents is based on proportional-resonant (PR) control where a single control loop is sufficient to regulate both sequence currents and to eliminate the 120 Hz ripples [3], [6], [7].

The two methods will be implemented into a solar PV's grid-connected converter. Furthermore, this paper carries out a side by side comparison study of the dynamic performance of the two types of unbalance control.

The paper is organized as follows. Section II describes the control design structures of the two unbalance control techniques for a VSC system. The EMT testbed description is demonstrated in Section III. Simulation results is presented in Section IV. Finally, Section V summarizes the major conclusions of the paper.

## II. CONTROL OF THREE-PHASE VSC UNDER UNBALANCED CONDITIONS

This section describes the two types of unbalance control for a grid-connected VSC system. The two control techniques are first studied based on their inner current loops where both positive- and negative- sequence currents are simultaneously regulated. Then, the sequence reference current generation and the outer loop regulators are described.

### A. Inner Current Control Loops

The distributed energy resources (DER) converter system in this paper is a standard three-phase two-level VSC, connected to a distribution network at its Point of Common Coupling (PCC) through a filter ( $Z_f = R_f + jX_f$ ), as shown in Fig.1.

The three-phase dynamic equation of VSC system connected to PCC is expressed in  $abc$  frame as follow.

$$v_{cabc} - v_{pccabc} = L_f \frac{di_{cabc}}{dt} + R_f i_{cabc} \quad (1)$$

where  $v_{cabc}$ ,  $i_{cabc}$ , and  $v_{pccabc}$  are three-phase output VSC voltages, currents, and the voltages at the PCC bus, respectively. (1) can be transformed to space vector form as in (2).

$$\vec{V}_c - \vec{V}_{pcc} = L_f \frac{d\vec{I}_c}{dt} + R_f \vec{I}_c \quad (2)$$

Besides, the space vectors can be then represented either in stationary frame ( $\alpha\beta$  frame) or synchronous reference frame (SRF) ( $dq$  frame). At steady state,  $dq$  components are DC quantities, while  $\alpha\beta$  components are sinusoidal quantities.

### 1) Double Inner Control Loops:

The quantities vectors in (2) can be represented in double  $dq$  frames as the sum of positive and negative sequence vectors, such that,  $\vec{V}_c = V_{c,dq}^+ e^{j\omega t} + V_{c,dq}^- e^{-j\omega t}$  where  $\omega$  is the angular frequency. The first term indicates the positive components rotating in counterclockwise whose angle frequency is  $\theta^+ = +\omega t$ . The second term denotes the negative components rotating in clockwise with  $\theta^- = -\omega t$ . Thus, (2) can be formed in positive  $dq^+$  and negative  $dq^-$  frames. The transformed decomposed subsystems of the positive and negative sequence dynamics equations are expressed in (3) and (4), respectively

$$V_{c_d}^+ - V_{pcc_d}^+ = R_f I_{c_d}^+ + L_f \frac{dI_{c_d}^+}{dt} - \omega L_f I_{c_q}^+ \quad (3)$$

$$V_{c_q}^+ - V_{pcc_q}^+ = R_f I_{c_q}^+ + L_f \frac{dI_{c_q}^+}{dt} + \omega L_f I_{c_d}^+$$

$$V_{c_d}^- - V_{pcc_d}^- = R_f I_{c_d}^- + L_f \frac{dI_{c_d}^-}{dt} + \omega L_f I_{c_q}^- \quad (4)$$

$$V_{c_q}^- - V_{pcc_q}^- = R_f I_{c_q}^- + L_f \frac{dI_{c_q}^-}{dt} - \omega L_f I_{c_d}^-$$

Dynamic expressions in (3)-(4) are first order-linear systems where controlled currents  $I_{c,dq}^+$  and  $I_{c,dq}^-$  are coupled by  $\omega L_f$ . As a result, two control loops for each sequence frame are required in order to simultaneously regulate both positive- and negative-sequence currents. Each loop contains two PI controllers (ability to track DC signals accurately with zero steady state error) as well as decoupling terms  $\omega L_f$  in order to achieve a decoupled control. Thus, the controlled positive- and negative-sequence voltages of the converter are expressed in (5) and (6), respectively.

$$\begin{aligned} V_{c_d}^+ &= u_d^+ + V_{pcc_d}^+ - \omega L_f I_{c_q}^+ \\ V_{c_q}^+ &= u_q^+ + V_{pcc_q}^+ + \omega L_f I_{c_d}^+ \end{aligned} \quad (5)$$

$$\begin{aligned} V_{c_d}^- &= u_d^- + V_{pcc_d}^- + \omega L_f I_{c_q}^- \\ V_{c_q}^- &= u_q^- + V_{pcc_q}^- - \omega L_f I_{c_d}^- \end{aligned} \quad (6)$$

where  $u_d^\pm = \Delta I_d^\pm (k_{pi} + \frac{k_{ii}}{s})$  and  $u_q^\pm = \Delta I_q^\pm (k_{pi} + \frac{k_{ii}}{s})$ .  $u_{dq}^\pm$  are the output of the PI controllers and  $\Delta I_{dq}^\pm$  is the errors between the reference and measurement currents. Fig. 3 shows the control diagram of the dual-sequence current controllers.

Note that when  $I_{c,abc}^+$  are measured and then transferred into  $dq$  quantities ( $dq^+$  and  $dq^-$  frames), both sequence

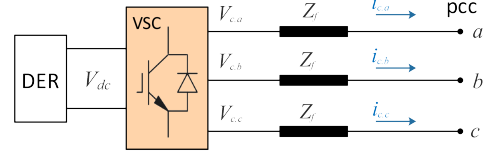


Fig. 1: Two-level three-phase VSC connected to PCC .

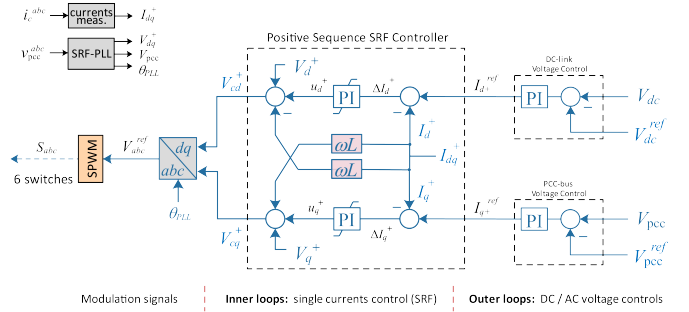


Fig. 2: Schematic control structure of a grid-connected VSC system regulating only the  $dq$  positive-sequence current, well-known as a conventional control (single SRF).

components interact with each other generating oscillations at 120 Hz (twice the fundamental frequency) during unbalanced conditions [8]. However, these ripples can not be cancelled by PI controllers due to its infinite gain of a dc input. Thus, since a  $2\omega$  cross-coupling effect exists between the sequence  $dq$  currents, a  $2\omega$  cross-decoupling terms as a feedback loop can be used to avoid the current oscillations [5].

### 2) Single Inner Control Loop:

Since (2) can be formed in  $\alpha\beta$  frame, the sum of positive and negative sequence vectors is such  $\vec{i}_c = i_{c_\alpha} + i_{c_\beta}$ . Thus, (2) can be formed as:

$$V_{c_\alpha} - V_{pcc_\alpha} = R_f I_{c_\alpha} + L_f \frac{di_{c_\alpha}}{dt} \quad (7)$$

$$V_{c_\beta} - V_{pcc_\beta} = R_f I_{c_\beta} + L_f \frac{di_{c_\beta}}{dt} \quad (8)$$

It can be seen that no coupling terms are presented in (7)-(8). Since signals presented in  $\alpha\beta$ -frame have a sinusoidal form, two proportional+resonant controllers (PR controllers) are able to concurrently track both positive and negative currents in a single control loop. Hence, the converter voltage in  $\alpha\beta$ -frame can be expressed as.

$$V_{c_\alpha} = u_\alpha + V_{pcc_\alpha} \quad (9)$$

$$V_{c_\beta} = u_\beta + V_{pcc_\beta} \quad (10)$$

where

$$u_\alpha = \Delta I_\alpha (k_p + \frac{2k_r}{s^2 + \omega_0^2})$$

$$u_\beta = \Delta I_\beta (k_p + \frac{2k_r}{s^2 + \omega_0^2})$$

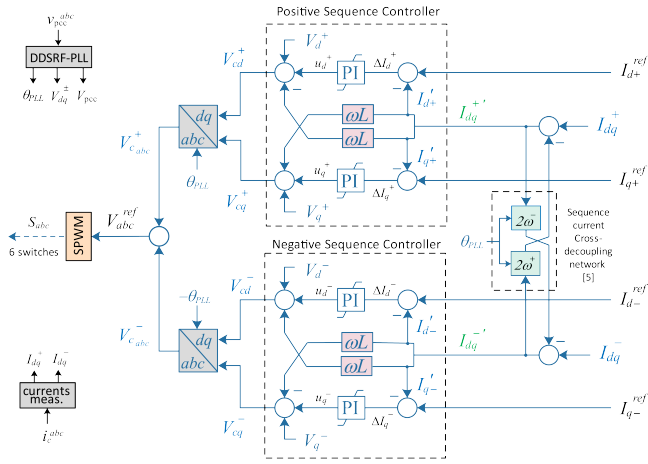


Fig. 3: Schematic control structure of a grid-connected VSC system using decoupled double synchronous reference frame (DDSRF) current controllers.

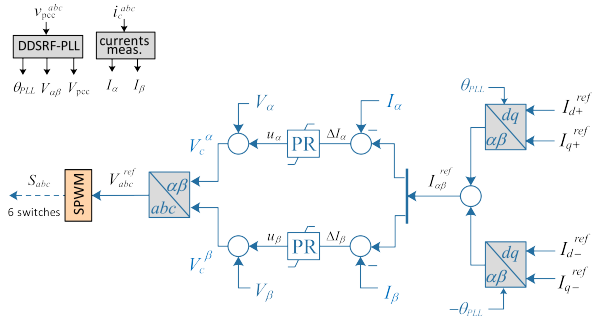


Fig. 4: Schematic control structures of a VSC in a grid-connected system using PR current controllers.

$\omega_0$  is the resonant frequency. A control diagram of PR controllers in a single current loop controlling sequence currents is depicted in Fig. 4.

Note that this control aims not only to control positive and negative currents, but also to avoid the double frequency by its regulators. Since a PR regulator has infinity gain at a certain frequency, it can achieve a zero steady state error at that frequency.

### B. Current Reference Generation

There is a need to calculate suitable positive and negative reference currents to be commanded to such current control loops of Fig. 3 and Fig. 4. Thus, these reference values are basically obtained based on the active and reactive power. The instantaneous complex power at PCC is well-known as.

$$S_{\text{PCC}} = v_{\text{PCC}} i_c^* = P_{\text{PCC}} + jQ_{\text{PCC}} \quad (11)$$

The power expressed in terms of transformed positive-negative sequences of voltages and currents ( $dq^+$  and  $dq^-$  frames) are written as follow.

$$S_{\text{PCC}} = (V_{dq}^+ e^{j\omega t} + V_{dq}^- e^{-j\omega t})(I_{dq}^+ e^{j\omega t} + I_{dq}^- e^{-j\omega t})^* \quad (12)$$

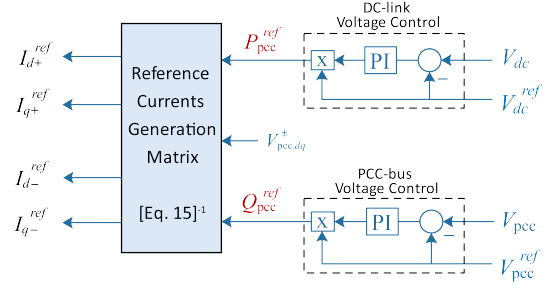


Fig. 5: The implementing of the outer loops; DC and AC voltage controllers in order to generate powers commands, then to the positive and negative reference currents generation.

The real part of (12) represents the active power, whereas, the imaginary part indicates the reactive power as shown in (13)-(14), respectively.

$$P(t)_{\text{PCC}} = P_0 + P_{c2} \cos(2\omega t) + P_{s2} \sin(2\omega t) \quad (13)$$

$$Q(t)_{\text{PCC}} = Q_0 + Q_{c2} \cos(2\omega t) + Q_{s2} \sin(2\omega t) \quad (14)$$

where  $P_0$  and  $Q_0$  are the average values of the active and reactive powers delivered into the grid, respectively.  $P_{c2}$ ,  $P_{s2}$ ,  $Q_{c2}$  and  $Q_{s2}$  are second order harmonic terms of these instantaneous powers. These harmonic components generate ripples in active and reactive power under unbalanced voltage dips.  $Q_{c2}$  and  $Q_{s2}$  can be neglected because they do not affect the oscillating active power; hence they do not need to be regulated.

$$\begin{bmatrix} P_0 \\ Q_0 \\ P_{c2} \\ P_{s2} \\ Q_{c2} \\ Q_{s2} \end{bmatrix} = \begin{bmatrix} V_d^+ & V_q^+ & V_d^- & V_q^- \\ V_q^+ & -V_d^+ & V_q^- & -V_d^- \\ V_d^- & V_q^- & V_d^+ & V_q^+ \\ V_q^- & -V_d^- & -V_q^+ & V_d^+ \\ V_q^- & -V_d^- & V_q^+ & -V_d^+ \\ -V_d^- & -V_d^- & V_d^+ & V_q^+ \end{bmatrix} \begin{bmatrix} I_d^+ \\ I_q^+ \\ I_d^- \\ I_q^- \end{bmatrix} \quad (15)$$

The power components in (13) and (14) expressed in terms of transformed positive- and negative-sequences of voltages and currents can be formed in a  $6 \times 4$  matrix as shown in (15) [3], [6]. Since  $Q_{c2}$  and  $Q_{s2}$  are ignored, (15) can be converted into a  $4 \times 4$  matrix. Therefore, the sequence current references can be determined by taking the inverse of (15).  $P_{c2}$  and  $P_{s2}$  are set to zero to obtain proper reference currents. In this paper,  $P_0$  and  $Q_0$  are defined to  $P_{\text{PCC}}^{\text{ref}}$  and  $Q_{\text{PCC}}^{\text{ref}}$  that are obtained from the outer loops as discussed in the next section, respectively.

It should be emphasized that the positive and negative reference commands generating from (15) will be implemented to both types of unbalance control in Fig. 3 and Fig. 4. In Fig. 4, the  $dq$  reference orders are required to be transferred into  $\alpha\beta$  frame. Thus, the sum of  $I_{\alpha\beta+}^{\text{ref}}$  and  $I_{\alpha\beta-}^{\text{ref}}$  provides the aggregated reference commands to the PR controllers.

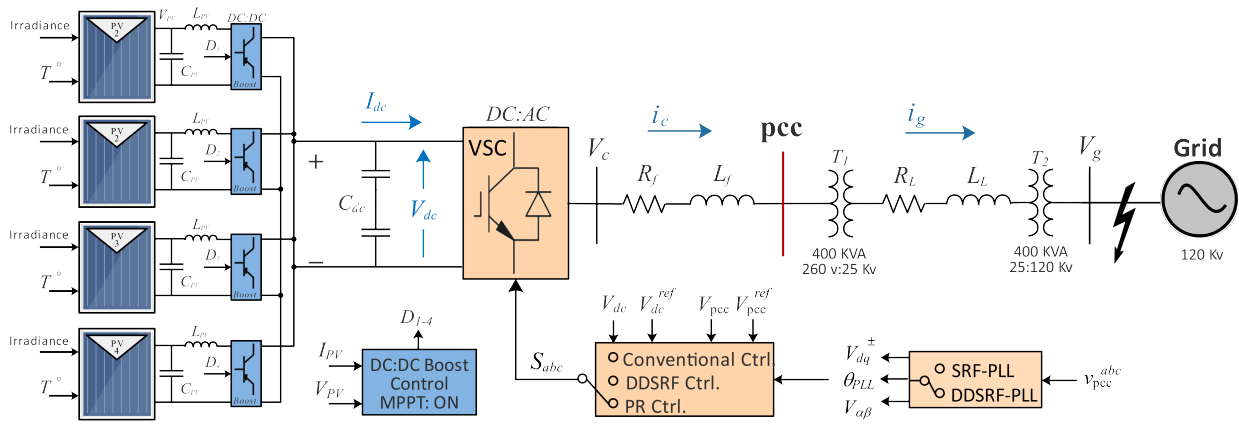


Fig. 6: The EMT testbed of 400-KW PV Farm connected to a grid when different control techniques of a VSC are implemented.

### C. Outer Loops Control

For a grid-connected VSC, when only positive-sequence components is regulated, the active current reference is obtained from the DC-link voltage controller, while the reactive current reference is obtained from the ac voltage controller [9] [10]. However, When regulating both positive- and negative-sequence components, the DC-link and PCC voltages are no longer controlled by only the positive current and voltages sequences but also by negative sequences components.

(16) represents power balance in the DC-link capacitor at steady state operation, where  $P_{pv}$  is the output power of the PVs, and  $V_{pcc} I_{c_d}$  is the output power of the converter in per unit. Therefore, the reference active power  $P_{pcc}^{ref}$  can be determined by controlling the DC voltage as shown in Fig. 5. In addition, the reactive power reference  $Q_{pcc}^{ref}$  is obtained based on (17) by regulating the PCC voltage (assuming a PCC voltage aligned  $dq^+$ -frame, i.e.,  $V_d^+ = 1$  and  $V_q^+ = 0$  pu). These reference powers stand for the average powers ( $P_0, Q_0$ ) in (15), respectively.

$$V_{dc} I_{dc} = P_{pv} - V_{pcc,d} I_{c_d} \quad (16)$$

$$Q_{pcc} = -V_{pcc,d} I_{c_q} \quad (17)$$

Note also due to the relationship in (16), the DC-link voltage control assumes positive feedback control since the voltage decreases if the real power export increases. Whereas, the AC voltage control assumes a negative feedback control in (17).

## III. EMT TESTBEDS DESCRIPTION

### A. System Description

The EMT testbed used in this paper, as shown in Fig. 6, is a three-phase grid-connected PV system developed in MATLAB/SimScape environment. The PV farm is composed of four PV arrays connected in parallel and each PV array produces a maximum power at 100 kW at a sun irradiance of  $1000 \text{ W/m}^2$ . The PV arrays are interfaced a two-level VSC through a DC/DC boost converter for each array operated at maximum power point tracking (MPPT)-perturb and observe

Table I: The PV testbeds and different types of VSC system control parameters.

	Description	Symbol	Value
Grid side	Transformer 1	$T_1$	400 kVA 260 V \ 25 kV
	Transformer 2	$T_2$	400 kVA 25 kV \ 120 kV
	Transmission line	$R_L, X_L$	$X_L/10, 0.2$ pu
	System frequency	$f$	60 Hz
DER side	Rated power	S	400 kVA
	ac voltage	$V_{ac}$	260 V
	DC-link voltage	$V_{dc}$	500 V
	VSC filter	$R_f, X_f$	$X_f/50, 0.156$ pu
	DC-link capacitor	$C_{dc}$	0.02 F
	PV inductor	$L_{pv}$	5 mH
PV capacitor	$C_{pv}$	100 $\mu$ F	
VSC control system	Outer voltage loops	DC-voltage Ctrls	$k_{pp}, k_{ip}$
		PCC-voltage Ctrls	$k_{pv}, k_{iv}$
		Single SRF Ctrls	$k_{pp}, k_{ip}$
	Inner current loops	DDSRF Ctrls	$k_{pi}, k_{ii}$
		PR Ctrls	$k_p, k_r$
	SRF-PLL	PI controllers	$k_p, k_i$
	DDSRF-PLL		60, 1400

algorithm. The VSC system is connected to a grid at PCC-bus of 260 V through a filter ( $R_f, X_f$ ). Two Y ground Y ground transformers ( $T_1, T_2$ ) step up the 260 V to a 25 kV transmission line and then to a 120 kV grid bus.

In order to evaluate the performance of the presented VSC current control techniques in grid-connected PV during unbalanced grid conditions, three EMT testbeds are provided. In testbed 1, the VSC control is performed in a conventional control where positive sequence is only regulated (i.e. single reference frame), such illustrated in Fig. 2. In testbeds 2 and 3, the VSC control implements in DDSRF control and PR control where both positive- and negative-sequence are controlled.

### B. Grid Synchronization System

Due to the need of the grid synchronization system, two different phase locked loop (PLL) are used in this paper. The grid voltage phase angle is usually detected by a conventional synchronous reference PLL (SRF-PLL) detector for balanced cases [11]. The SRF-PLL is applied to testbed 1. However,

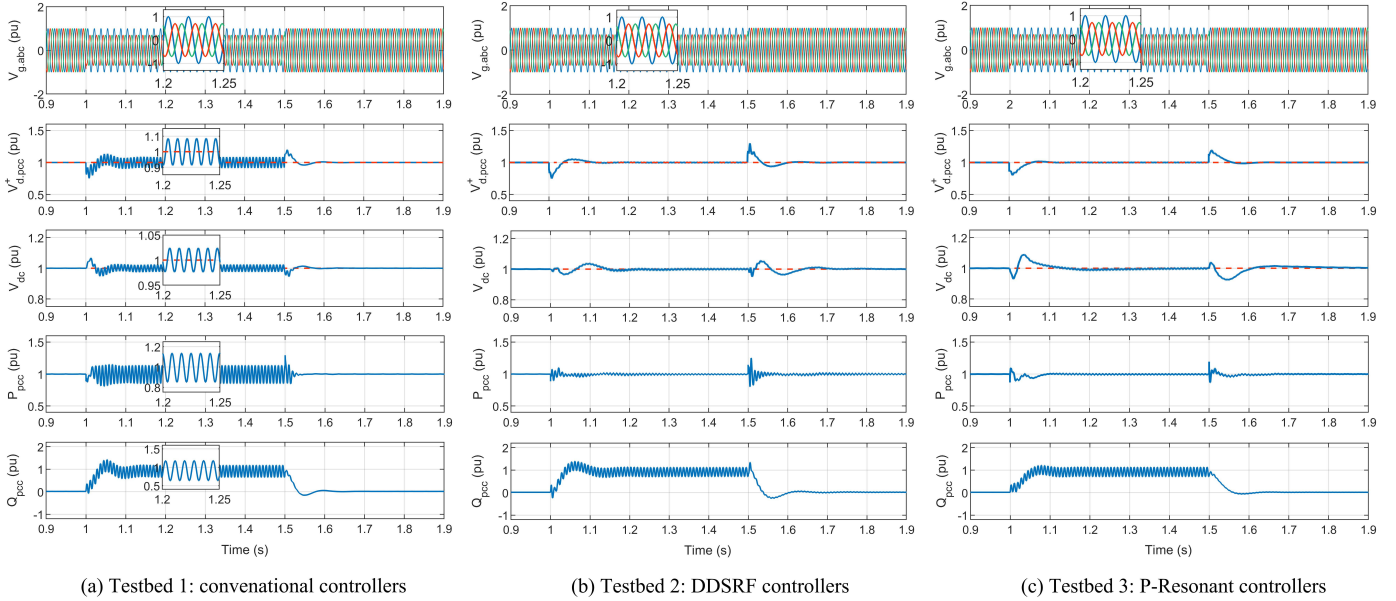


Fig. 7: Simulation responses for different VSC current controls. (7a) conventional control (7b) DDSRF control (7c) p-resonant control. The results shows (top-bottom) the three-phase grid voltage, PCC-bus voltage, DC-link voltage, PCC active and reactive power. Event: grid voltage subjects to unbalance fault at 1 sec. "Solid line" denotes measured quantity, while "dashed line" refers reference command.

when a grid subjects to unbalance, the conventional PLL does not operate properly because the detected angle has low frequency oscillations. Thus, as an alternative, a decoupled DDSRF-PLL can be used. The DDSRF-PLL is not only able to extract the phase angle accurately, but also to eliminate the  $2\omega$  ripples from the input of the PLL's controller (i.e.  $V_q^+ = 0$  pu). This PLL is suitable for unbalance control, hence it is implemented in testbeds 2 and 3 [6], [12].

#### IV. SIMULATION RESULTS

For all simulation cases, a line-to-line fault with 30% voltage dip in phases  $a$  and  $b$  is applied at the grid side during the time period from  $t = 1$  sec to 1.5 sec. In addition, the reference orders for the DC-link and AC voltages ( $V_{dc}^{ref}$ ,  $V_{pcc}^{ref}$ ) are commanded to 1 pu. For fast simulation speed, average model for the VSC is adopted.

##### A. Testbed 1: conventional control

Fig. 2 illustrates the conventional VSC control where positive sequence is only regulated, i.e. single reference frame. Fig. 3(a) shows the simulation results of three-phase grid voltage, positive  $d$  voltage magnitude, DC-link voltage, and the injected active and reactive powers into the grid.

The DC-link voltage and PCC-bus voltage can follow their respective commands. However, the ac voltage generates an oscillation at double the fundamental grid frequency that cannot be avoided by the SRF-PLL. The DC voltage has also a ripple of  $2\omega$ . Such the ripple is comparatively small, but it gives rise to oscillations in the active power, as shown in the figure.

##### B. Testbed 2: DDSRF control

In this testbed, the VSC control is performed in unbalance control mode, that is, DDSRF control in which both positive- and negative-sequence currents are regulated.

It can be seen from Fig. 3(b) that both the DC-link and PCC voltages are able to rapidly track their corresponding reference orders. Note the 120 Hz ripple in the AC voltage is eliminated by the DDSRF-PLL. Also, the DDSRF current control is able to mitigate the ripples in the active power and DC voltage.

Fig. 8 provides clear illustrations of the dynamic performance of the measured converter current in  $abc$  frame and sequence ( $dq^+$  and  $dq^-$ ) frames (solid lines). It is obvious that both positive- and negative-sequence currents are controlled and quickly follow their command values (dashed lines).

##### C. Testbed 3: P-resonant control

Testbed 3 carries out unbalance control for VSC system that employs the PR control of Fig. 4, where sequence currents are regulated.

Fig. 7(c) confirms that the DC-link and PCC voltage controllers have the ability to track the reference commands at zero steady state. Fig. 9 shows the measured converter current in  $abc$  frame and reference  $\alpha\beta$  frame (solid lines). Obviously, the PR controllers are not only able to effectively follow their respective commands (dashed lines), but also they are able to cancel out the  $2\omega$  ripples. Thus, the oscillations in the DC-link voltage and the injected real power are mitigated.

Finally, it can be concluded that both types of VSC unbalance control; DDSRF and PR controls, achieve a perfect performance in controlling positive- and negative-sequence current and mitigating the 120 Hz ripples in the active power.

## V. CONCLUSION

In this paper, two types of unbalance control techniques are implemented in the grid-connected converter of a solar PV to not only regulate DC-link voltage and AC voltage, but also mitigate double frequency ripples in the total power being delivered into the grid. Simulation results of MATLAB/SimScape testbeds validate the feasibility of the unbalance controls. The testbeds are compared side by side for their dynamic behavior.

## REFERENCES

- [1] G. Kou, L. Chen, P. VanSant, F. Velez-Cedeno, and Y. Liu, "Fault characteristics of distributed solar generation," *IEEE Transactions on Power Delivery*, vol. 35, no. 2, pp. 1062–1064, 2019.
- [2] R. Kabiri, D. G. Holmes, and B. P. McGrath, "Control of active and reactive power ripple to mitigate unbalanced grid voltages," *IEEE Transactions on Industry Applications*, vol. 52, no. 2, pp. 1660–1668, 2015.
- [3] R. Teodorescu, M. Liserre, and P. Rodriguez, *Grid converters for photovoltaic and wind power systems*. John Wiley & Sons, 2011, vol. 29.
- [4] H.-S. Song and K. Nam, "Dual current control scheme for pwm converter under unbalanced input voltage conditions," *IEEE transactions on industrial electronics*, vol. 46, no. 5, pp. 953–959, 1999.
- [5] M. Reyes, P. Rodríguez, S. Vázquez, A. Luna, J. M. Carrasco, and R. Teodorescu, "Decoupled double synchronous reference frame current controller for unbalanced grid voltage conditions," in *2012 IEEE Energy Conversion Congress and Exposition (ECCE)*. IEEE, 2012, pp. 4676–4682.
- [6] M. Mirhosseini, J. Pou, B. Karanayil, and V. G. Agelidis, "Resonant versus conventional controllers in grid-connected photovoltaic power plants under unbalanced grid voltages," *IEEE Transactions on Sustainable Energy*, vol. 7, no. 3, pp. 1124–1132, 2016.
- [7] R. Teodorescu, F. Blaabjerg, M. Liserre, and P. C. Loh, "Proportional-resonant controllers and filters for grid-connected voltage-source converters," *IEE Proceedings-Electric Power Applications*, vol. 153, no. 5, pp. 750–762, 2006.
- [8] M. Mirhosseini, J. Pou, and V. G. Agelidis, "Current improvement of a grid-connected photovoltaic system under unbalanced voltage conditions," in *2013 IEEE ECCE Asia Downunder*. IEEE, 2013, pp. 66–72.
- [9] A. Yazdani and R. Iravani, *Voltage-sourced converters in power systems: modeling, control, and applications*. John Wiley & Sons, 2010.
- [10] A. Alsaif, Z. Miao, and L. Fan, "Comparison of islanding and synchronization for a microgrid with different converter control," in *2019 North American Power Symposium (NAPS)*. IEEE, 2019, pp. 1–6.
- [11] L. Fan, *Control and dynamics in power systems and microgrids*. CRC Press, 2017.
- [12] P. Rodríguez, J. Pou, J. Bergas, J. I. Candela, R. P. Burgos, and D. Boroyevich, "Decoupled double synchronous reference pll for power converters control," *IEEE Transactions on Power Electronics*, vol. 22, no. 2, pp. 584–592, 2007.

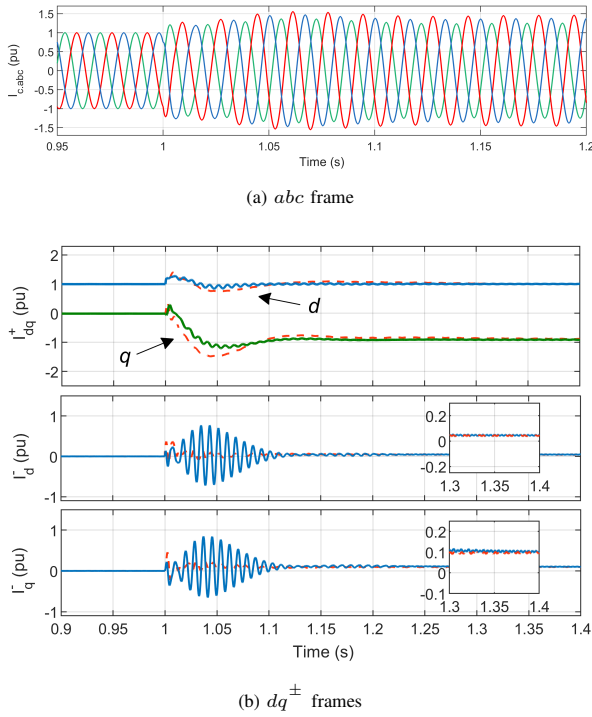


Fig. 8: Dynamic responses of the VSC output current during unbalanced grid conditions. (8a) the measured three-phase currents. (8b) the controlled positive- and negative-sequence currents in  $dq^\pm$  frames.

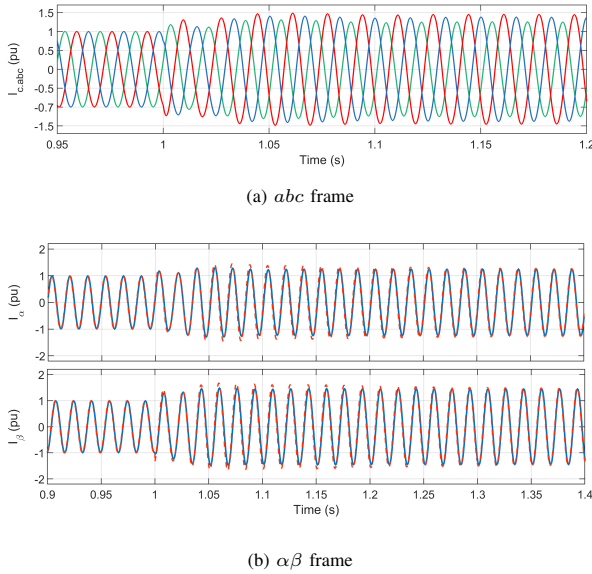


Fig. 9: Dynamic responses of the VSC output current during unbalanced grid conditions. (9a) the measured three-phase currents. (9b) the controlled currents in  $\alpha\beta$  frame.

Note that the use of PR controllers enhances relatively the dynamic performance of the grid-connected VSC system since no need to separate positive- and negative-sequence components for the current control loops; compared to the DDSRF current control..